Atmospheric Environment 213 (2019) 25–36

Contents lists available at ScienceDirect

Atmospheric Environment

journal homepage: www.elsevier.com/locate/atmosenv

Trend reversal from high-to-low and from rural-to-urban ozone concentrations over Europe

Yingying Yan[a,*], Jintai Lin[b], Andrea Pozzer[c], Shaofei Kong[a], Jos Lelieveld[c]

[a] Department of Atmospheric Sciences, School of Environmental Studies, China University of Geosciences (Wuhan), 430074, Wuhan, China
[b] Laboratory for Climate and Ocean-Atmosphere Studies, Department of Atmospheric and Oceanic Sciences, School of Physics, Peking University, Beijing 100871, China
[c] Atmospheric Chemistry Department, Max Planck Institute for Chemistry, Mainz, Germany

ARTICLE INFO

Keywords:
Ozone trends
Urban
Rural
Model simulation

ABSTRACT

The trends per 5th percentile interval of European surface ozone concentrations over urban, suburban and rural sites in the period 1995–2012 have been estimated based on observational data from the European Environment Agency air quality database. Consistent with previous study results, we find a rapid decline of relatively high ozone concentrations after the year 1995, especially of rural summertime ozone. However, the decreasing rate has slowed, and even reversed, of low-level ozone, especially in the urban environment for all seasons. Although the ozone air pollution problem has been declared to be effectively resolved by achieving European air quality goals, our results indicate that ozone remains to be difficult to control for a long time into the future. Global and regional models poorly reproduce the measured differences in ozone and trends in different levels and regions. Thus policy guidelines from the model should be considered with care.

1. Introduction

Tropospheric ozone plays a key role in atmospheric environment as it initiates free radical chain reactions which oxidize many trace gases, and it is a powerful greenhouse gas (Monks et al., 2015). Thus, even a small change of ozone concentrations could have significant effects in the oxidation capacity and the energy budget of the troposphere (Yan et al., 2016). It is also a secondary pollutant which has detrimental effects on human health and crop yields (Lelieveld et al., 2015; Fleming et al., 2018). In recent years, progressively lower concentrations of the health damage threshold level (Office of Air and Radiation, EPA, 2014) have been estimated, based on growing evidence from clinical (Kim et al., 2011) and epidemiological (Bell et al., 2014) studies. The European Union (EU) Air Quality Directive lowered the standard in 2008 to 120 μg/m^3 for the maximum daily 8-hourly average (MD8A) ozone concentrations relative to the 1992 ozone directive (180 μg/m^3 for 1 h average concentration; https://www.eea.europa.eu/publications/TOP08-98/page006.html/).

From the 1990s–2010s, regional pollution emission controls in Europe focused on VOCs and NO_x sources such as fossil fuel combustion by power plants as well as motor vehicles, leading to a continuous decline in European anthropogenic emissions (Derwent et al., 2010; Jenkin, 2008; Derwent and Hjellbrekke, 2013). As a result of the precursor emission reduction, a decreasing trend in the peak summertime ozone concentrations over rural regions (Jonson et al., 2006; Lefohn et al., 2017; Yan et al., 2018b) and in the number of exceedances with respect to the standard (Guerreiro et al., 2014) have been identified from measurements over EuropeAlthough ozone concentrations are typically higher over rural than urban regions due to the local consumption of ozone (NO titration) in urban areas, the EEA (2017) has reported that 90% of the urban population is exposed to ozone exceeding the WHO guideline. Moreover, multiple evidence is provided by many studies (Sicard et al., 2013; Paoletti et al., 2014; Escudero et al., 2014; García et al., 2014; Querol et al., 2014, 2016) that show an increase in urban ozone, probably because of a lower NO titration effect associated with the reduction of NO emissions relative to NO_2. It has also been reported that regional rural ozone levels have changed little and remained approximately constant over the last two decades, although acute peak-level episodes have been drastically reduced compared to the late 1990s (EEA, 2017; Querol et al., 2016). In addition, the response of ozone to the anthropogenic emission change is locally dependent on the pollutant mix due to the nonlinearity in photochemical formation of ozone as a function of precursor concentrations (Monks et al., 2015; Lin et al., 2017; Xue et al., 2014). Thus, the trends diversity among urban, suburban and rural areas deserves being investigated further in view of the continuous decline in European anthropogenic emissions. It is important for better understanding of ozone changes and thus short-term policy and decision making.

* Corresponding author.
E-mail address: yanyingying@cug.edu.cn (Y. Yan).

https://doi.org/10.1016/j.atmosenv.2019.05.067
Received 11 January 2019; Received in revised form 23 May 2019; Accepted 27 May 2019
Available online 28 May 2019

Most previously reported changes in European ozone tended to focus on the maximum daily 8-h average (MD8A) ozone concentrations during the spring-to-summer season (Colette et al., 2011; Wilson et al., 2012; Guerreiro et al., 2014), which limited the understanding of ozone changes during different times of the day and seasons. Yan et al. (2018b) noticed the contrasting trends in the diurnal cycle of seasonal ozone measured across rural Europe. Their results showed a reduction in rural ozone during most times of day in the warm season, in contrast to the increases at night and in winter. Indeed, there are many studies related to the trends of the 5th, 50th, and 95th percentile ozone (Cooper et al., 2012; Colette et al., 2011; Wilson et al., 1996). These reports have shown an increasing trend in low-level (5th percentile) ozone concentrations over European sites. However, from a human health perspective, an increase in any level ozone concentrations enhances the potential health risk from long-term exposure to ozone, especially in view of the reported progressively lower ozone damage threshold (Brauer et al., 2013), and even the possibility that there is no safe threshold for health effects (Bell et al., 2006; Yang et al., 2012; Peng et al., 2013). Thus, the changes in ozone from high to low levels (every 5th percentile) deserve being discussed in more detail.

Here we analyze the measurement records from the European air quality database network (AirBase). We calculate the trends for each 5th percentile ozone mixing ratios using a statistical trend model. Ozone trends are shown for annual and seasonal averaged daytime and nighttime means over urban, suburban and rural sites. Furthermore, global chemistry-climate model ECHAM5/MESSy (EMAC) simulations and regional model simulations based on GEOS-Chem European nested grid are conducted to primarily evaluate the model abilities in capturing the observed ozone trends per 5th percentile among the urban, suburban and rural sites and the response of ozone to the continuous decline in European anthropogenic emissions.

2. Datasets and methods

2.1. Ozone measurements

The focus of the present work is to study the overall changes in European ozone at different levels and various regions. Measurements at regulatory air quality monitoring stations, conducted in the 1990s and including hundreds of sites with records close to or longer than 20 years, constitute the main data source. The data are hourly ground-level ozone observations during 1995–2012 obtained from the European Environmental Agency's (EEA) public air quality database 'AirBase' (https://www.eea.europa.eu/data-and-maps/data/airbase-the-european-air-quality-database-7). The volume and diversity of the data offer an unprecedented view into ozone trends over Europe with stations representing from urban to rural background air characteristics. AirBase contains a multi-annual time series of air quality monitoring data and statistics submitted by participating countries throughout Europe. It is used to produce assessments of air quality covering the whole geographical area of Europe. Colette et al. (2011) (study period: 1998–2007) and Wilson et al. (1996) (study period: 1996–2005) performed such assessments, reaching the conclusion of an enhancement in ozone at urban sites and non-significant changes over rural background regions. These two studies further show that, considering daily peaks but not daily means, less sites with an increasing ozone trend are measured. Derwent and Hjellbrekke (2013) further demonstrated that ozone mixing ratios over urban areas are gradually getting close to the levels of rural regions, hence reinforcing the results of Colette et al. (2011), indicating an increased upwards trends at urban stations. However, their results show that the previous reported opposite trend for background and peak ozone (Vautard et al., 2006; study period: 1990–2002; with remote EMEP stations) do not hold using AirBase dataset.

In general, in the Airbase database, the available observation sites are ranging from 371 (125 urban sites, 95 suburban sites and 151 rural sites) in 1995 to 888 (418 urban sites, 188 suburban sites and 282 rural sites) in 2008, and the percentage of missing hourly data in individual year varies between 3.3 and 13.5% for urban, suburban and rural regions (Table 1). As the surface air quality monitoring networks are often designed for population exposure and regulatory purposes rather than trend assessment, and the temporal consistency of the data is a major concern in trend studies. Fortunately, the monitoring networks have improved significantly since 1998 following a change in legislation. For this work, the consistency of the dataset is ensured by excluding the sites that do not fulfill the data selection criteria put forward by Cooper et al. (2012) and further applied by Yan et al. (2018a, b) for long-term ozone trends analysis: (1) excluding the monitoring days when the missing hourly data covers more than 4 h during nighttime or daytime; (2) excluding the specific season that contains valid data < 60 days; (3) for each season, when the valid seasonal mean ozone reports are more than 13 years between 1995 and 2012, we keep the data in all years for the particular season, otherwise we discard. This criterion is more relevant for trend calculation than that derived from the guidelines of the European Environmental Agency (EEA, 2009; Colette et al., 2011). The finally selected stations that satisfy the above criteria for the analysis amount to a total of 685 sites (Fig. 1) including 289 urban sites, 150 suburban sites and 246 rural sites.

Table 1
Number of European urban, suburban and rural sites, and percentages of missing hourly data in each year in the Airbase station observations.

Year	Urban		Suburban		Rural	
	Sites num.	Missing data	Sites num.	Missing data	Sites num.	Missing data
1995	125	3.7%	95	4.4%	151	5.9%
1996	138	7.0%	98	4.9%	167	5.3%
1997	186	6.8%	123	5.3%	210	7.9%
1998	210	8.3%	135	9.8%	226	5.9%
1999	407	13.5%	186	9.8%	275	7.4%
2000	399	7.1%	183	6.9%	272	4.4%
2001	409	6.9%	183	7.0%	272	4.4%
2002	382	6.9%	179	6.4%	273	4.4%
2003	389	6.3%	178	6.5%	271	4.4%
2004	407	6.1%	183	6.2%	277	4.7%
2005	407	7.8%	185	6.5%	279	4.8%
2006	412	6.3%	189	5.6%	281	3.7%
2007	406	6.7%	189	4.6%	279	3.5%
2008	418	5.7%	188	5.0%	282	3.2%
2009	414	5.6%	188	5.1%	281	3.4%
2010	417	8.2%	187	5.6%	282	4.2%
2011	381	7.5%	181	6.3%	268	3.5%
2012	367	8.4%	172	5.4%	261	3.3%

To investigate the changes in overall ozone air quality over Europe, we calculated the trends for the annual and seasonal European ground level ozone of each 5th percentile for daily (24 h) mean, daytime (local time: 0700–1900h) mean and nighttime (local time: 1900–0700 h) mean values over urban, suburban and rural sites, respectively. The monthly individual 5th percentile ozone mixing ratios for diurnal, daytime and nighttime are calculated from the hourly ozone concentrations in the relevant period (diurnal, daytime and nighttime) in individual month. The monthly values are further used for ozone trend calculations.

We used a statistical trend model (Yoon and Pozzer, 2014; Yan et al., 2018b) with monthly time series (Y_t) data to perform the calculation of trends considering diurnal mean, daytime mean and nighttime mean ozone. This linear trend model has the form of $Y_t = \mu + S_t + \omega X_t + N_t$, where μ represents the offset and is a constant component, ω is the estimated trend per year for calculating data, $X_t = t/12$ (with t as month) represents the time index term, and N_t is the unexplained noise term in the trend estimates. S_t indiactes the seasonal variation. We performed the trend estimation with the deseasonalized monthly ozone data using a simple trend model of the form:

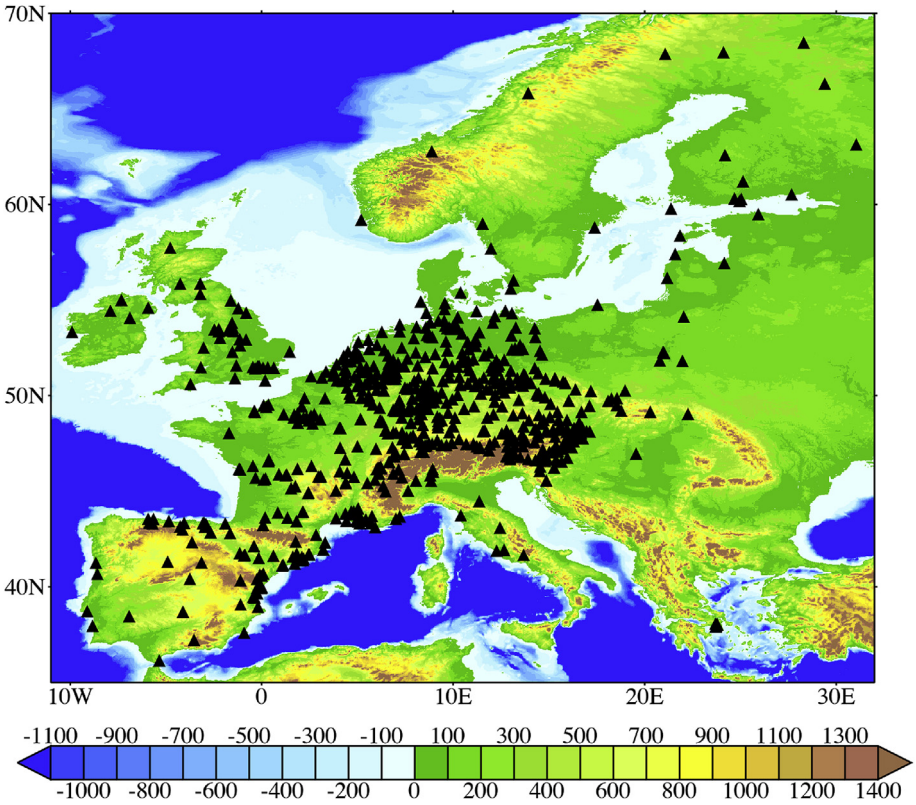

Fig. 1. Site distribution of the selected 685 sites (1995–2012) for the airbase datasets. The overlaid map shows the surface elevation (m) from a 2 min Gridded Global Relief Data (ETOPO2v2) available at NGDC Marine Trackline Geophysical database (http://www.ngdc.noaa.gov/mgg/global/etopo2.html).

$Y_t = \mu + \omega X_t + N_t$. The seasonal component does not affect much the statistical characteristics of the other terms in the model (Weatherhead et al., 1998; Yoon and Pozzer, 2014), although this component is essential in practical modeling of monthly surface ozone time series.

To test the sampling bias of ozone trends against the data selection criteria, we further applied two alternate criteria to choose sites following Yan et al. (2018a). SI Appendix Sect. S1 details how we processed data from the observation sites to justify the robustness of ozone trends presented here. Table S1 shows that, for the European annual mean ozone, ozone trends of our default data selection criteria are similar to those from the two alternate criteria with the growth rates of 0.51–0.56 μg/m^3/y for urban ozone, 0.19–0.22 μg/m^3/y for suburban ozone, and −0.01–0.02 μg/m^3/y for rural ozone. We thus conclude that our ozone trends results are robust against our choice of sites and data.

2.2. Model simulations

2.2.1. Global EMAC model simulation

Surface ozone mixing ratios during the 1995–2012 periods are simulated using the ECHAM5/MESSy2 (5th generation European Centre Hamburg general circulation model, version 5.3.02/2nd Modular Earth Submodel System, version 2.51) Atmospheric Chemistry (EMAC) model (Roeckner et al., 2006; Jöckel et al., 2016). EMAC simulated ozone and its precursor gas-phase tracers have been extensively evaluated in previous studies (e. g. Pozzer et al., 2012; Yan et al., 2018b).

The model results were obtained with a T42 spherical representation (approximately 2.8 latitude by 2.8 longitude corresponding to a quadratic Gaussian grid), and 90 levels in the vertical (the top level up to 0.01 hPa). The chemical mechanism (Mainz Isoprene Mechanism version 1) used in the simulations includes 310 reactions of 155 species (ozone, odd nitrogen, methane, alkanes, alkenes and halogens, etc.). In EMAC simulations, monthly anthropogenic and biomass burning emissions are adopted from the MACCity (Monitoring Atmospheric Composition & Climate/City Zero Energy) emission inventory (Eyring et al., 2013), incorporated as prescribed sources following the Chemistry-Climate Model Initiative (CCMI) recommendations. The total non-methane volatile organic compounds (NMVOCs) are calculated from the corresponding species for anthropogenic sectors with the MACCity raw dataset (Jöckel et al., 2016). Emissions from natural sources (lightning NO_x, soil NO_x, biogenic isoprene, terrestrial dimethyl sulfide (DMS), volcanic SO_2, halocarbons and ammonia) have been parameterized and calculated online based on climatologies. Further details of the model setup (emissions and chemical processes) are described as the RC1SD-base-10a simulation in Jöckel et al. (2016), conducted by the ESCiMo project. In order to compare model results with hourly observations, we re-run the RC1SD-base-10a simulation in Jöckel et al. (2016) with EMAC model to cover the full period of measurements and also with a 1-hourly temporal resolution for ozone.

2.2.2. Regional GEOS-Chem model simulations

Regional model simulations of surface ozone based on the GEOS-Chem European nested grid (http://acmg.seas.harvard.edu/geos/; version 11-01) have been conducted to study the simulated contrast of ozone changes among the urban, suburban and rural sites. The model was run at a horizontal resolution of 0.625° long. X 0.5° lat. with 47 vertical layers, as driven by the MERRA-2 meteorological fields provided by the Global Modeling and Assimilation Office (GMAO) at NASA Goddard Space Flight Center. The model is run with the tropospheric HO_x-NO_x-hydrocarbon-aerosol-bromine plus methyl peroxy nitrate chemistry.

Base inventories of anthropogenic precursor emissions are from EMEP (Auvray and Bey, 2005; available at http://www.ceip.at/). The EMEP inventory is only available for 1995–2005. In order to simulate the interannual variability of pollutants in the following years, we scaled the EMEP NO_x, SO_2 and CO emissions from the base year (2005) to other years between 2006 and 2012, based on the annual MACCity

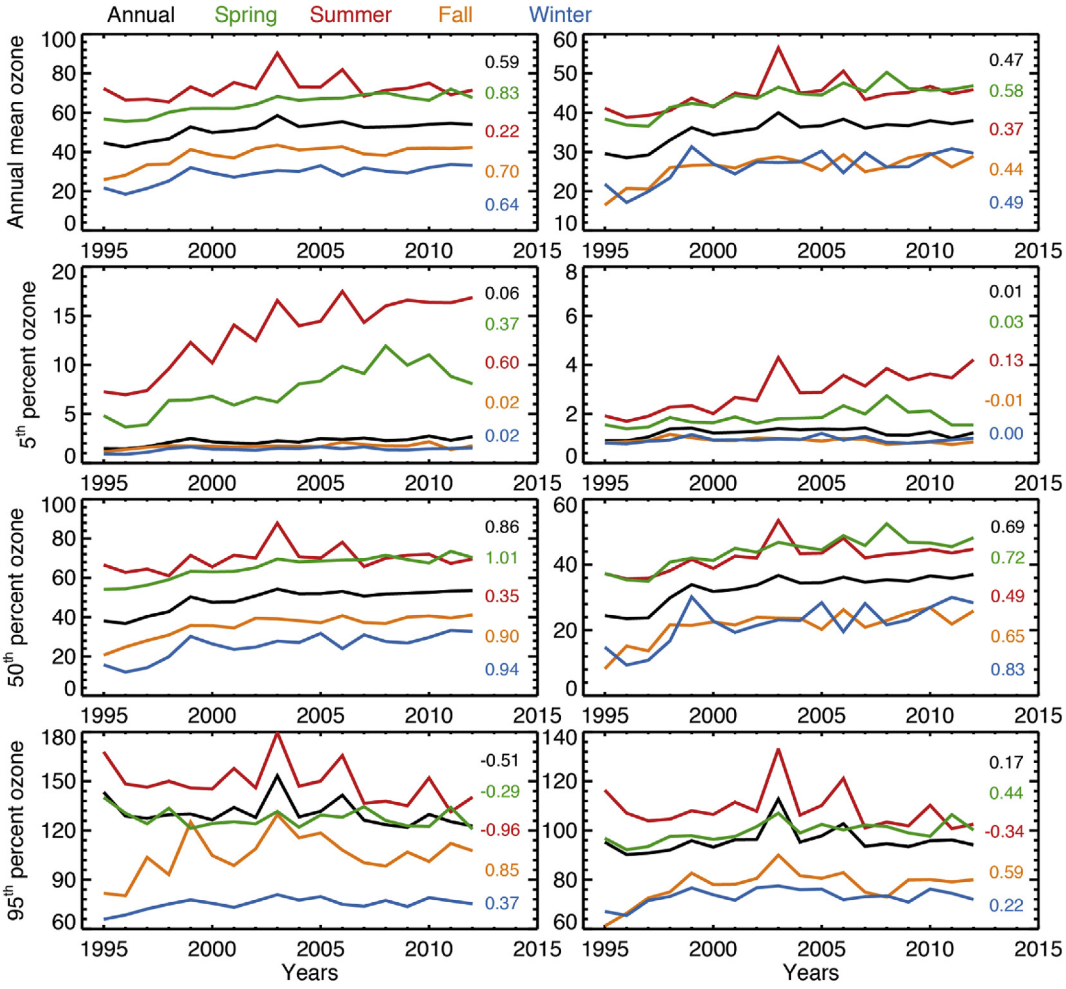

Fig. 2. Annual and seasonal mean daytime (left panels) and nighttime (right panels) ozone mixing ratios (μg/m^3) averaged over the urban sites for mean (first row), 5th (second row), 50th (third row), and 95th (forth row) percentiles. Also shown in each panel are the trends (μg/m^3/y).

emissions (http://eccad.sedoo.fr/eccad_extract_interface/JSF/page_login.jsf). Biomass burning emissions use the Global Fire Emissions Database version 4 (GFED4) data. Other natural emissions (lightning NO_x, soil NO_x, and biogenic NMVOC) are parameterized in the model.

To illustrate the response of ozone to the continuous decline in European anthropogenic emissions, we have further conducted a sensitivity simulation with constant anthropogenic emission throughout the years. Limited by the computational resources, we only conducted nested grid simulations from 15 June through 31 July of each year, with results analyzed for July.

3. Ozone trends diversity among European urban, suburban and rural sites

3.1. Annual and seasonal ozone time series

Annual and seasonal mean, 5th, 50th, and 95th percentile daytime and nighttime ozone concentrations during 1995–2012 averaged over urban, suburban and rural sites are shown in Figs. 2–4, respectively. Ozone concentrations are shown to reach a minimum during the fall-to-winter season and a maximum in the spring-to-summer season at all types of sites including urban, suburban and rural stations. For annual mean ozone at different levels (black lines in Figs. 2–4), the mixing ratios over rural stations are higher than those at the suburban and urban sites both during daytime and at night. For all types of sites, the inter-annual variability is observed to be not very large with the exception of strongly enhanced ozone during 2003 (ozone anomalies in excess of 36 μg/m^3 in 2003 relative to 2012). For mean ozone, the sharp increase by up to 21 μg/m^3 in the year 2003 occurred during a strong European heat wave (Tressol et al., 2008; Solberg et al., 2008; Ordóñez et al., 2010; Yan et al., 2018b).

3.2. Ozone trends over urban and suburban sites

For the urban sites, annual and seasonal mean ozone has increased rapidly with the statistically significant growth rates of 0.22–0.83 μg/m^3/y (P-value < 0.01 under an F-test; Fig. 2 and Table 2) during 1995–2012. These ozone enhancements are less but also significant over suburban stations (0.09–0.42 μg/m^3/y; P-value < 0.01), except that a decline rate of −0.19 μg/m^3/y (P-value < 0.01) is also found for suburban summertime mean ozone. Ozone enhancements over suburban and urban sites are stronger during daytime (0.20–0.83 μg/m^3/y for annual and seasonal means; P-value < 0.01) than at night (0.09–0.58 μg/m^3/y). The European suburban and urban ozone increases in mean values are mainly attributed to the rapid increasing trends in 50th percentile ozone (0.16–0.70 μg/m^3/y for suburban sites and 0.35–1.01 μg/m^3/y for urban sites). In addition, the ozone increases of suburban and urban spring-to-summer 5th percentile (0.37–0.60 μg/m^3/y at urban, and 0.36–0.52 μg/m^3/y at suburban) during daytime also contribute much to the enhancement in mean ozone. Such increasing seasonal ozone average concentrations in the 5th percentile ozone at urban sites have also been reported in various previous studies (Yan et al., 2018a; Lin et al., 2017; Cooper et al., 2012; Paoletti et al., 2014; Sicard et al., 2016), especially for springtime

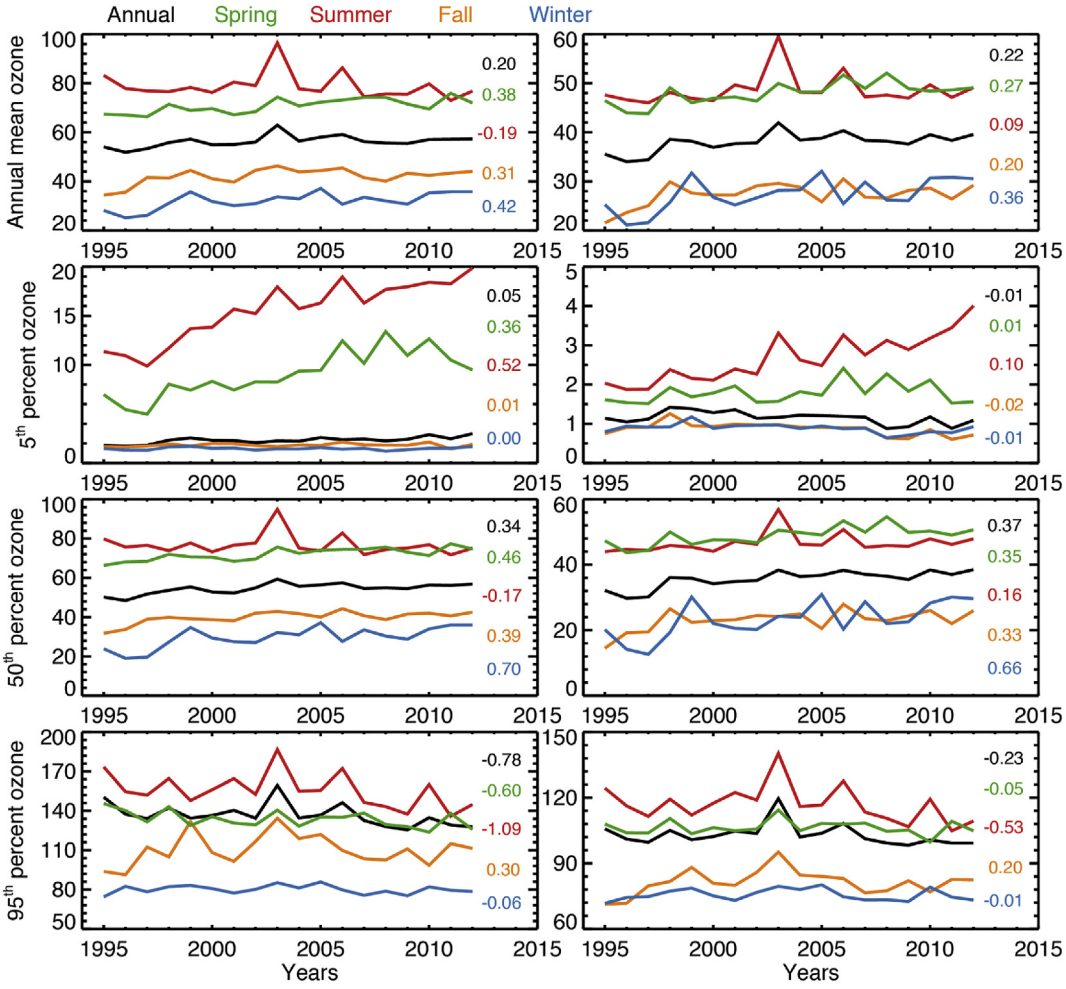

Fig. 3. Annual and seasonal mean daytime (left panels) and nighttime (right panels) ozone mixing ratios (μg/m^3) averaged over the suburban sites for mean (first row), 5th (second row), 50th (third row), and 95th (forth row) percentiles. Also shown in each panel are the trends (μg/m^3/y).

ozone. The 5th percentile ozone enhancements in spring are probably partially due to an increase of the global background ozone mixing ratios (Ziemke et al., 2018; Parrish et al., 2017; Wang et al., 2009) and partially attributed to a reported shift of the seasonal cycle in ozone in the northern hemisphere (Parrish et al., 2013; Cooper et al., 2014; Clifton et al., 2014; Simon et al., 2015). The sharp decreasing trends in summertime 95th percentile at urban (-0.96 μg/m^3/y, P-value $<$ 0.01) and suburban (-1.09 μg/m^3/y, P-value $<$ 0.01) sites compensate the increasing trends in 5th and 50th percentiles, leading to moderate enhancement over urban (0.22 μg/m^3/y) and slight decline over suburban (-0.19 μg/m^3/y) sites in summer.

Fig. 5 further shows the trends in annual ozone concentrations (mean, 5th, 50th and 95th percentile) over urban and suburban sites during the 1995–2012 period, for each hour of the day. For the urban sites, while the 5th percentile ozone does not show significant trends, the average ozone concentrations (and 50th percentiles) show significant increasing trends, and 95th percentile ozone show trends with a clear diel cycle (increasing at night and decline in daytime). The decreasing trend of 95th percentile ozone is most pronounced (-0.9 ± 0.6 μg/m^3/y; P-value $<$ 0.01) during the afternoon (1600–1800 h). 95th percentile ozone concentrations show an increasing trend during the night, however the trends are observed to be smaller (0.3 ± 0.4 μg/m^3/y; P-value $<$ 0.01) with a maximum in the morning (0800–0900 h; 0.5 ± 0.4 μg/m^3/y). This maximum in the morning is probably related to the rush hour, and the ozone enhancements may be tied to the increasing usage of diesel passenger cars in the past two decades (Zervas et al, 2006a,b). In contrast to the 95th percentile, the mean (50th percentile) ozone over urban sites shows an increasing trend especially during the morning (0.9 ± 0.35 μg/m^3/y; P-value $<$ 0.01). The standard deviation illustrates the variability of the trends among the stations, and therefore reflects the almost homogeneous decrease in 95th percentile ozone and increase in 50th percentile ozone over urban sites. Compared to the urban sites, suburban sites show similar shapes but lower values in trends for each percentiles.

3.3. Ozone trends over rural sites

In contrast to the enhancements in suburban and urban mean ozone, no trends for annual mean rural ozone (0.0 μg/m^3/y in daytime and -0.02 μg/m^3/y at night) are observed, with slight decreases and increases (-0.40 – 0.24 μg/m^3/y; an increasing trend for winter ozone and a decreasing trend for summer ozone) in seasonal mean ozone. Moreover, for seasonal ozone changes, increasing trends in rural 50th percentile (0.01–0.30 μg/m^3/y) are smaller than at suburban and urban sites (Table 3); declining trends in rural 95th percentile (-0.05 to -1.19 μg/m^3/y) are larger compared to suburban and urban regions (Table 2). The rapid deceasing trend in rural summer peak ozone is consistent with earlier reports of the long-term decrease in European surface ozone over the past two decades (Wilson et al., 1996; Yan et al., 2018b; Colette et al., 2011). These ozone decreases are a consequence of the continued decline in European anthropogenic ozone precursor emissions through EU regulations (Yan et al., 2018b; Cooper et al., 2012).

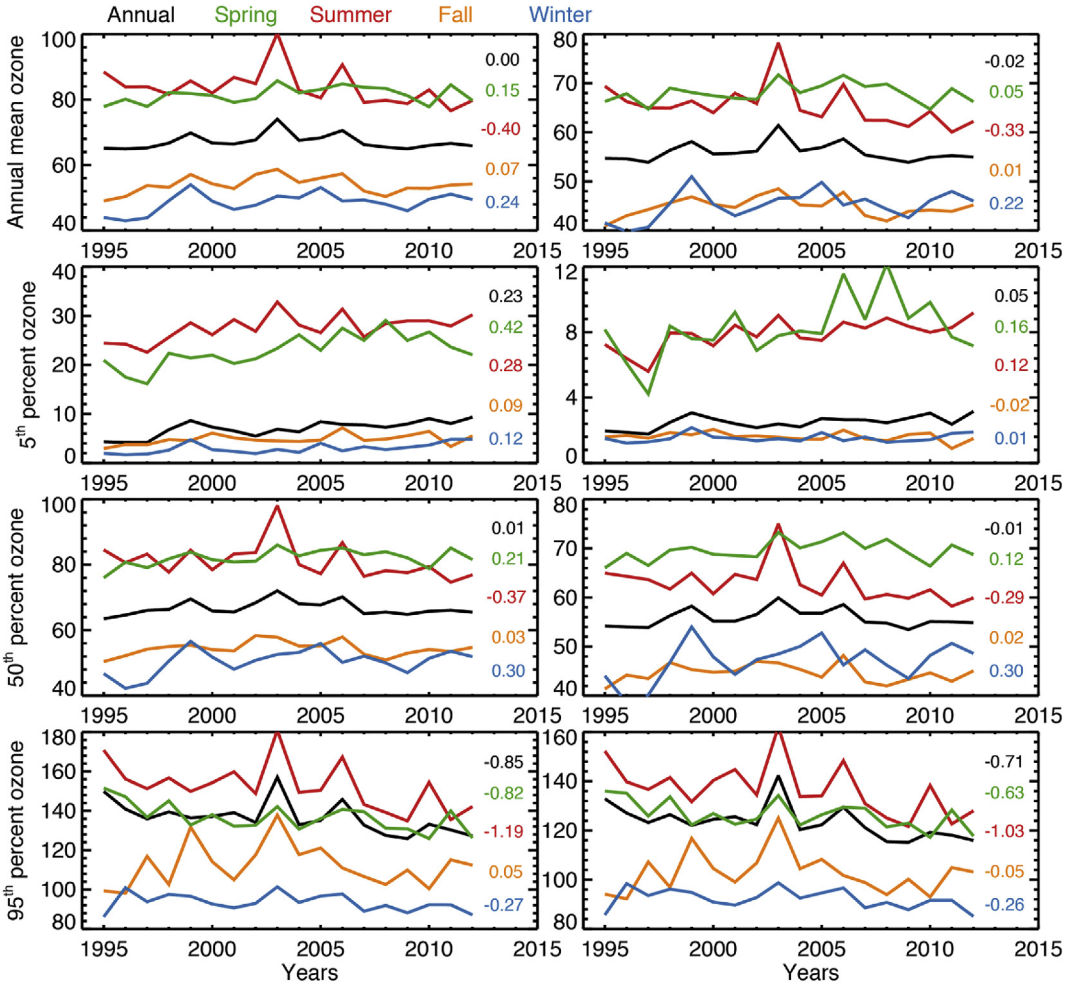

Fig. 4. Annual and seasonal mean daytime (left panels) and nighttime (right panels) ozone mixing ratios (μg/m^3) averaged over the rural sites for mean (first row), 5th (second row), 50th (third row), and 95th (forth row) percentiles. Also shown in each panel are the trends (μg/m^3/y).

For trends of each hour per day in annual ozone concentrations (mean, 5th, 50th and 95th percentile), the averages (and 50th percentiles) do not show significant trends. The 5th percentile ozone shows significant trends only during the hours of the ozone photochemical buildup (1000–1800 h). The 95th percentile ozone shows a decreasing trend during the 1995–2012 period with the trend being most pronounced (-1.1 ± 0.7 μg/m^3/y; P-value < 0.01) during afternoon (1600–1700 h). 95th percentile ozone concentrations also show a decreasing trend during the night, however the trends are observed to be smaller (-0.7 ± 0.6 μg/m^3/y; P-value < 0.01).

3.4. Ozone trends for each 5th percentile

The trends per 5th percentile interval for the 1995–2012 European annual and seasonal daytime and nighttime mean ozone are presented in Fig. 6 and Fig. S1, respectively. For daytime mean ozone, the AirBase data yield statistically significant declining trends in high-level ozone (P-value < 0.01), especially for 95th percentile rural summer ozone.

Table 2
Observed linear trends[1] of the 1995–2012 European mean annual and seasonal averaged daytime and nighttime mean as well as the 5th, 50th and 95th percentile ozone concentrations.

	Seasons	Mean			5th percentile			50th percentile			95th percentile		
		urban	suburban	rural	urban	suburban	rural	urban	suburban	rural	urban	suburban	rural
Daytime (μg/m^3/y)	Annual	0.59**	0.20*	0.00	0.06	0.05	0.23*	0.86**	0.34**	0.01	−0.51**	−0.78**	−0.85**
	MAM	0.83**	0.38**	0.15*	0.37**	0.36**	0.42**	1.01**	0.46**	0.21*	−0.29**	−0.60**	−0.82**
	JJA	0.22*	−0.19*	−0.40**	0.60**	0.52**	0.28*	0.35**	−0.17*	−0.37**	−0.96**	−1.09**	−1.19**
	SON	0.70**	0.31**	0.07	0.02	0.01	0.09	0.90**	0.39**	0.03	0.85**	0.30**	0.05
	DJF	0.64**	0.42**	0.24*	0.02	0.00	0.12	0.94**	0.70**	0.30**	0.37**	−0.06	−0.27*
Nighttime (μg/m^3/y)	Annual	0.47**	0.22*	−0.02	0.01	0.01	0.05	0.69**	0.37**	−0.01	0.17*	−0.23*	−0.71**
	MAM	0.58**	0.27*	0.05	0.03	0.01	0.16*	0.72**	0.35**	0.12	0.44**	−0.05	−0.63**
	JJA	0.37**	0.09	−0.33**	0.13	0.10	0.12	0.49**	0.16*	−0.29*	−0.34**	−0.53**	−1.03**
	SON	0.44**	0.20*	0.01	−0.01	−0.02	0.02	0.65**	0.33**	−0.02	0.59**	0.20*	−0.05
	DJF	0.49**	0.36**	0.22*	0.00	−0.01	0.01	0.83**	0.66**	0.30**	0.22*	−0.01	−0.26*

1. ** P-value < 0.01. * P-value < 0.05 under an *F*-test.

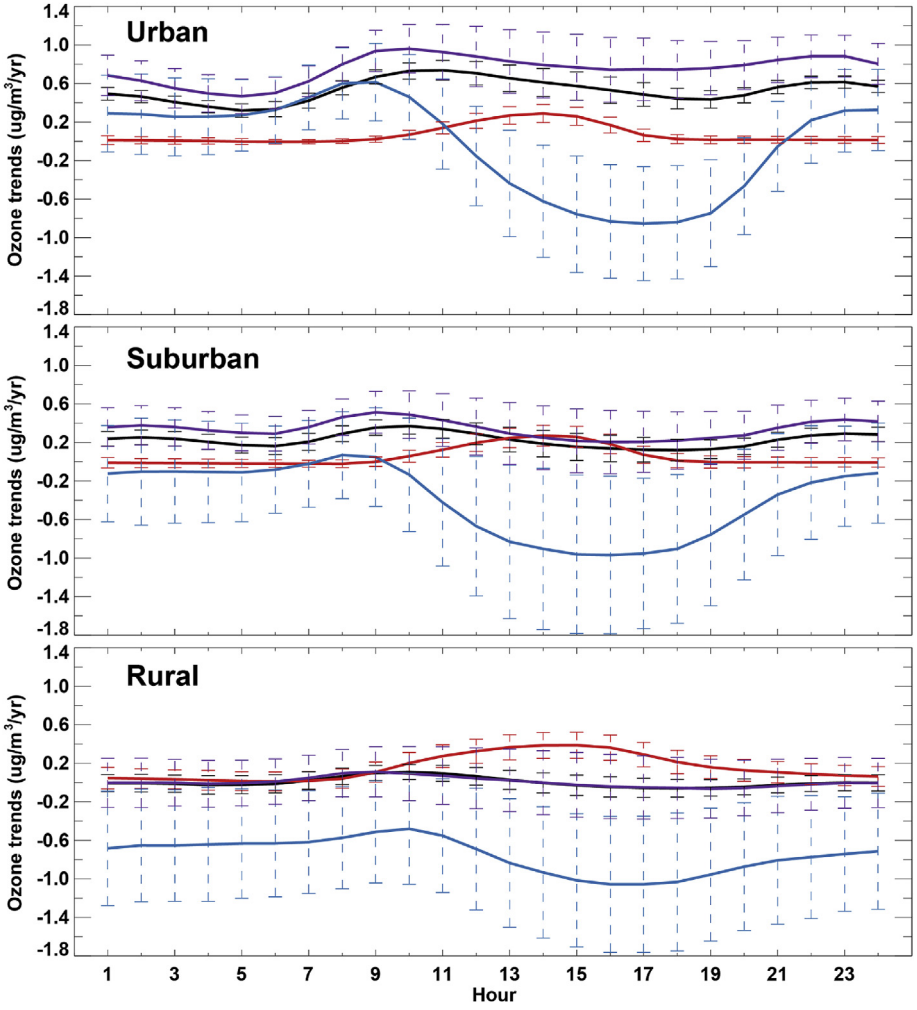

Fig. 5. Trend in the observed surface ozone averaged over urban, suburban and rural sites. The black line shows the 1995–2012 linear trends in the deseasonalized monthly ozone anomalies for each hour of the day (local standard time), the red, purple and blue lines depict the observed trend for 5th, 50th and 95th percentile ozone, respectively, and the dashed bars indicate their standard deviations. (For interpretation of the references to colour in this figure legend, the reader is referred to the Web version of this article.)

However, the declining trend has slowed from high to low ozone levels, and even reversed to an increasing one in the low-level ozone (Fig. 6). The trend shapes of nighttime mean ozone are similar but with smaller trends than those in daytime mean ozone (Fig. S1). From spring to winter, the most pronounced increases for seasonal European ozone are shown in the low level (10th to 15th percentiles) to middle level (50th percentile) ozone concentrations.

Over rural stations, almost all summer percentiles follow a decreasing trend and their significance increases with the ozone concentrations. However, winter rural ozone concentrations follow an increasing trend, being statistically most significant at lower ozone levels (P-value $<$ 0.01). The contrasting trends for seasonal rural ozone lead to near-zero trends in the annual means. The ozone increasing trends that occur in the warm season over rural sites are weaker and opposite for suburban and urban sites. The increases in the cold season are statistically significant (P-value $<$ 0.01) and are becoming more pronounced from rural to urban areas. Over urban sites, ozone concentrations are shown to follow an overall enhancement with statistically significant increases (P-value $<$ 0.01) for annual and seasonal means across the percentiles, except that a decrease is also visible in high level summer ozone ($>$ 80th percentile for daytime and $>$ 95th percentile for nighttime). For the annual mean ozone over suburban and urban areas, we find a statistically significant increasing trend (P-value $<$ 0.05). The results show that the overall ozone air quality over

Table 3
Modeled linear trends[a] of the 1995–2012 European mean daytime and nighttime mean as well as the 5th, 50th and 95th percentile ozone concentrations in July based on the GEOS-Chem nested simulation results.

	Seasons	Mean			5th percentile			50th percentile			95th percentile		
		urban	suburban	rural	urban	suburban	rural	urban	suburban	rural	urban	suburban	rural
Daytime (μg/m^3/y)	Control	0.17*	0.08	−0.22*	0.24**	0.22*	0.12*	0.32*	0.15	−0.19*	−0.18*	−0.41**	−0.49**
	Fixed emiss.	0.04	0.02	0.01	0.02	0.02	0.03	0.06	0.04	0.02	0.03	0.01	−0.02
Nighttime (μg/m^3/y)	Control	0.19*	0.09	−0.21*	0.17	0.16	0.07	0.33**	0.14	−0.16*	0.07	−0.19*	−0.46**
	Fixed emiss.	0.03	0.02	0.00	0.02	0.02	0.02	0.05	0.03	0.01	0.03	0.01	−0.04

[a] ** P-value $<$ 0.01. * P-value $<$ 0.05 under an *F*-test.

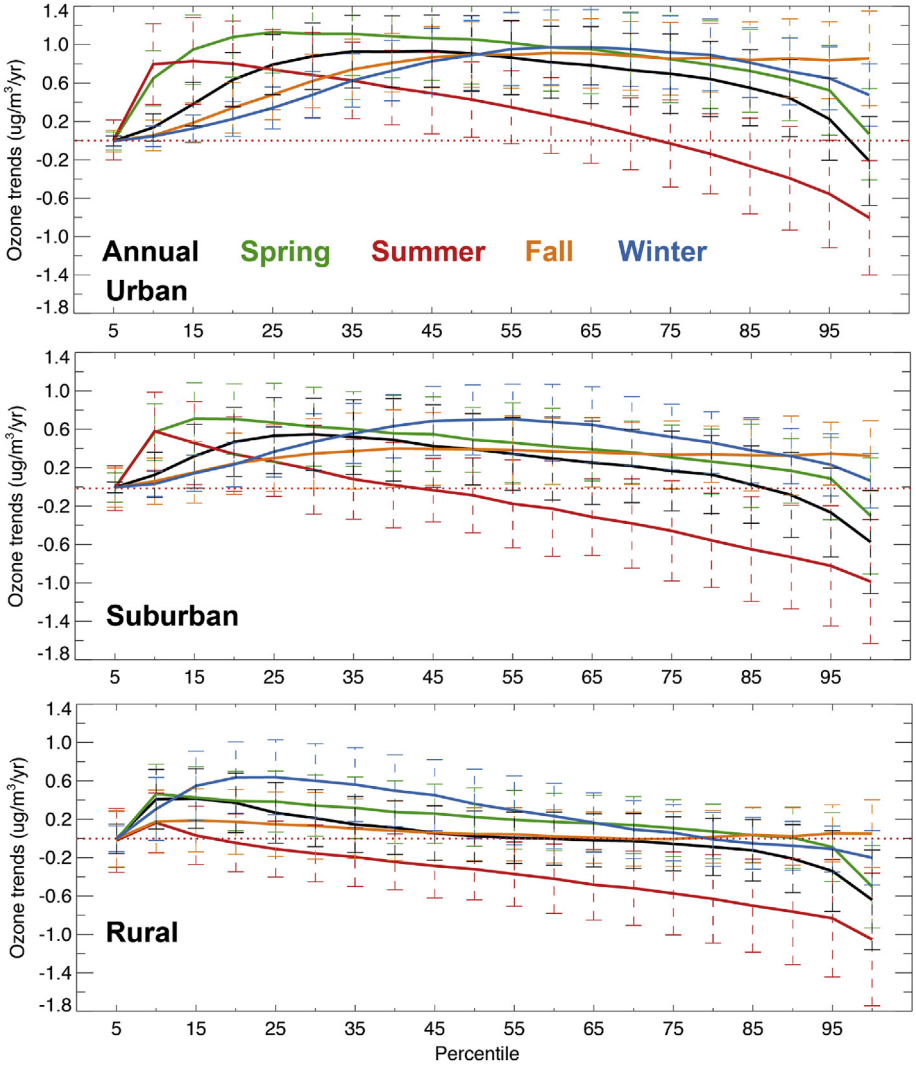

Fig. 6. Trends in observed daytime surface ozone averaged over Europe, calculated based on data from the urban, suburban and rural sites. The black line shows the 1995–2012 linear trends in the deseasonalized European monthly ozone anomalies for each 5th percentile, the green, red, yellow and blue lines depict the observed trend for seasonal ozone, and the dashed bars indicate their deviations. (For interpretation of the references to colour in this figure legend, the reader is referred to the Web version of this article.)

Europe has deteriorated especially in the urban regions.

3.5. Ozone exceedances among urban, suburban and rural sites

In view of the surface ozone mixing ratio limits in the European directive, we calculate the exceedance number for the public information threshold as well as the long-term objective (Fig. S2). Although both exceedances have declined over suburban (−2.3% for information threshold, −0.7% for long-term objective, P-value < 0.01) and rural (−3.0% and −0.7%, P-value < 0.01) regions, the exceedances for the long-term objective have become more numerous over urban (2.2%, P-value < 0.01) regions during 1995–2012. It may increase the risk of health effects from relatively lower ozone level exposure over urban regions, also considering the progressively reducing concentrations at which effects are expected (Brauer et al., 2013), and possible even no real lower threshold at which adverse health effects can be precluded (Peng et al., 2013). We note that the enhanced exceedances of the long-term objective over urban sites are in line with the increased annual mean ozone concentrations with the correlation of 0.67 (Fig. S2). Thus, to assess the effects of overall ozone changes on human health, we caution for focusing solely on trends calculated from MD8A or peak ozone mixing ratios, but also considering trends in mid-range and lower levels of ozone.

Overall, for different ozone levels, observed ozone concentrations at urban and suburban sites are close to the levels at rural sites. For all types of sites, the declining trend has slowed from high to low ozone levels, and even reversed to an increasing trend in low-level ozone. The reversal of long-term trends from high to low ozone levels or from rural to urban sites signifies the extent to which ground level ozone is locally or regionally controllable at all levels. Measures to effectively reduce peak ozone levels by controlling anthropogenic sources of VOCs and NO_x have been achieved, but defining policies for abating overall ozone air quality is much more challenging.

4. Simulated ozone trends

4.1. Global EMAC model simulated trends

The EMAC model results have been comprehensively compared to the observed ozone concentrations and trends at rural sites from the EMEP network (Yan et al., 2018b). During the 1995–2014 period, simulated results are highly correlated with observed monthly ozone (R = 0.84–0.91) with an overestimation (mean bias: 4.3 μg/m^3). The EMAC modeled ozone trends per hour also agree well with the

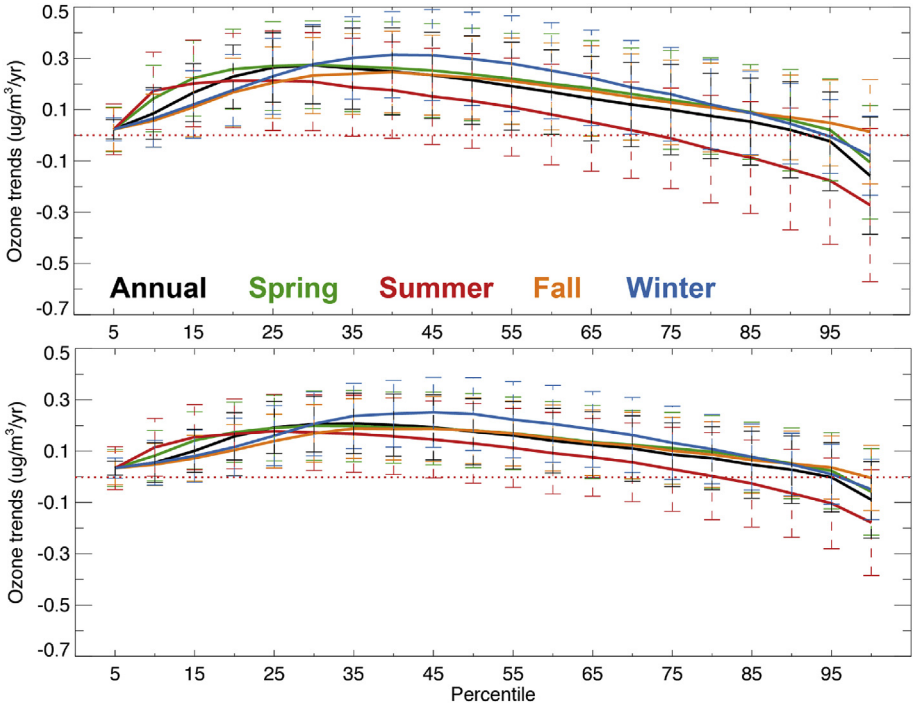

Fig. 7. Trends in global EMAC modeled daytime (top) and nighttime (bottom) surface ozone averaged over Europe. The black line shows the 1995–2012 linear trends in the deseasonalized European monthly ozone anomalies for each 5th percentile, the green, red, yellow and blue lines depict the observed trend for seasonal ozone, and the dashed bars indicate their deviations. (For interpretation of the references to colour in this figure legend, the reader is referred to the Web version of this article.)

observationally estimated diurnal cycle of the ozone trends. However, our EMAC model results are realized at coarse resolution, which could not reproduce the observed contrast ozone trends among the urban, suburban and rural sites. Here we focus on the analysis of trend reversal from high to low level ozone concentrations over the whole Europe.

The modeled trends in per 5th percentile daytime and nighttime surface ozone averaged over Europe are shown in Fig. 7. The EMAC model reproduces the observed trend reversal from high to low level ozone concentrations with statistically significant decreasing trends in high ozone levels and increasing trends in low-to-middle ozone levels. The model-observation correlation coefficients are 0.89–0.92 for the annual and seasonal ozone trends per 5th percentile. However, the modeled ozone trends (-0.6–$0.5\,\mu g/m^3/y$ for daytime and -0.4–$0.4\,\mu g/m^3/y$ for nighttime) are much lower than those derived from the measurements (-1.8–$1.6\,\mu g/m^3/y$ for daytime and -1.4–$1.2\,\mu g/m^3/y$ for nighttime) in all seasons. Moreover, the seasonal differences in modeled ozone trends are weaker than from observations. Parrish et al. (2014) compared results from three current chemistry–climate (ACCMIP) models and ozone measurements. It showed that the models can only capture ~50% of observed ozone changes, ~25–45% of the rate of changes, and little of the measured seasonal differences. These model biases are consistently identified in related findings by Staehelin et al. (2017), Young et al. (2018) and Lin et al. (2012, 2015, 2017). The discrepancies between modeled and observed ozone trends are attributed to factors including errors in the trends for anthropogenic precursor emissions (Hassler et al., 2016; Yan et al., 2018a,b) or poor representation of ozone changes due to natural sources, limits in resolving measured urban-rural diversity using coarse-resolution models (Yan et al., 2016; Lin et al., 2017) and more fundamental weaknesses in the model representation of the ozone-related processes.

4.2. Regional GEOS-Chem model simulated trends

Additional analysis of ozone trends in July during 1995–2012 was carried out using the nested GEOS-Chem model results. The GEOS-Chem modeled ozone trends per 5th percentile over urban, suburban and rural sites are shown in Fig. 8. The nested model reproduces the trend reversal from high to low level ozone concentrations. However, similar to the EMAC results, the GEOS-Chem model also tends to underestimate the observed ozone trends (Table 3). Further, the spatial differences in ozone trends among urban, suburban and rural sites (Fig. 8) are well captured by the nested model, although much smoother changes in trends of different percentiles are calculated from GEOS-Chem.

By fixing the anthropogenic emissions in 2012, we conduct a sensitivity simulation to show the response of ozone to the continuous decline in European anthropogenic emissions. With constant emissions, the modeled mean ozone shows a slight increase over urban, suburban as well as rural sites, in contrast to the trends (increasing trends over urban and suburban sites, but decreasing trends over rural sites) calculated from the control simulation (Table 3). In the sensitivity simulations no significant trend (less than $0.1\,\mu g/m^3/y$) for any percentile is found, and also no contrast in ozone trends among different percentiles and different types of sites (Fig. 8), which is well reproduced by the control simulation. Therefore, it appears that both the trend diversity in different percentile ozone and the spatial difference in ozone trends are associated with the rapid decline in the precursor gases anthropogenic emissions over Europe. Some evidence that reducing local or regional emissions can lead to an increase in 5th percentile and a decrease in 95th percentile ozone mixing ratios is provided by observational studies. The results indicate that increasing low-level (5th percentile) ozone occurred to a greater extent at more urbanized regions in Europe (Jenkin, 2008), at least partly because of changes in regional chemistry resulting from emission reductions rather than growth in global or regional background. Recent analyses of measurements and model simulations over Europe (Yan et al., 2018b) further indicate that reducing ozone precursor emissions may be partially responsible for the observed enhancements in the 5th percentile ozone over rural sites.

5. Discussion and conclusions

Reduction efforts in anthropogenic ozone precursor emissions over the past decades have shown to be effective in lowering peak ozone events over Europe, but the challenge to improve the overall local and regional ozone air quality has remained. Our results show that from peak to lower ozone levels, the observed decreasing trend in European ozone has weakened and even reversed in the period 1995–2012. This

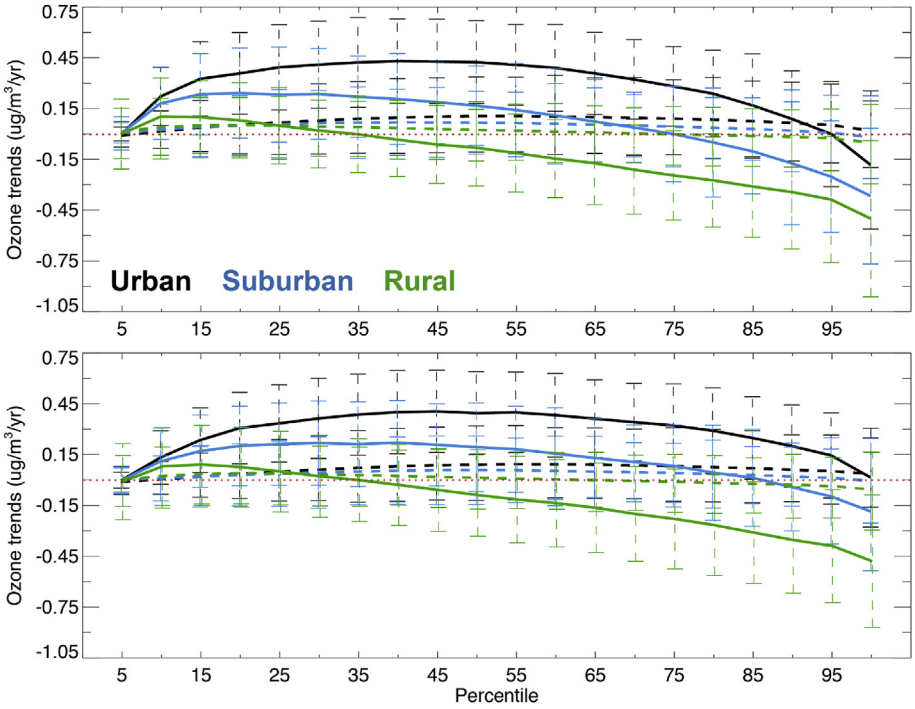

Fig. 8. Trends in regional GEOS-Chem modeled daytime (top) and nighttime (bottom) surface ozone in July of 1995–2012. The black line shows the linear trends in the urban ozone for each 5th percentile, the green, and blue lines depict the observed trend for rural and suburban ozone, and the dashed bars indicate their deviations. (For interpretation of the references to colour in this figure legend, the reader is referred to the Web version of this article.).

noteworthy change in different level ozone trends augments the difficulty to achieve the European air quality goals. We have further shown that the overall ozone air quality over Europe has deteriorated especially in the urban regions, associated with possibly enhanced health risks from long-term exposure to ozone in areas with high population density. Thus, efforts to further reduce emissions, necessary for Europe to achieve the standards, should consider not only the episodic peak ozone levels but also changes in overall ozone air quality.

Observed ozone levels at urban sites with high-NO_x environments are now increasing up to the levels observed over the rural regions surrounding them. These urban ozone enhancements are reportedly due to reduced ozone titration through chemical reaction with ambient nitric oxide, as a consequence of applying catalytic converters to the exhausts of diesel and petrol motor vehicles. The differences in ozone trends of individual percentiles between urban and rural areas in various seasons are primarily attributed to nonlinear chemistry in ozone production, responding to changes in local anthropogenic emissions. Thus, ozone pollution control efforts should involve locally-optimized solutions considering both the ozone production regime and emission status.

However, recent global and regional nested models do not reproduce the observed ozone changes well (Parrish et al., 2014; Derwent et al., 2016; Yan et al., 2018a,b). Moreover, model simulations of spatial differences in trends of different level ozone are challenging due to the complex and mutually dependent interactions of ozone related chemistry and physical processes (Lelieveld and Dentener, 2000; Lamarque et al., 2010; Yan et al., 2018a,b). Thus, the accuracy of European ozone trend estimates from using the models should be considered with caution. Further detailed analysis of the trends in different levels of ozone over urban, suburban and rural background regions should put forward additional critical tests of our understanding of the ozone-related processes as represented in current models.

Continued ozone observations and monitoring are needed to consolidate the evidence of ozone trends. Advanced chemistry-climate models with high horizontal resolution are needed to help improve our understanding of the nonlinear and spatio-temporally multi-scale ozone-emission-climate interactions that will have significant impacts on the future evolution of ozone and its role in air quality and climate change (Pawson et al., 2014; Yan et al., 2016; Young et al., 2018).

Acknowledgement

This study was financially supported by the Key Program of Ministry of Science and Technology of the People's Republic of China (2016YFA0602002; 2017YFC0212602). The research was also funded by the Fundamental Research Funds for the Central Universities, China University of Geosciences (Wuhan) (G1323519230) and the Start-up Foundation for Advanced Talents (162301182756). We acknowledge the free use of hourly ozone data from the European Environmental Agency's (EEA) public air quality database.

Appendix A. Supplementary data

Supplementary data to this article can be found online at https://doi.org/10.1016/j.atmosenv.2019.05.067.

References

Auvray, M., Bey, I., 2005. Long-range transport to Europe: seasonal variations and implications for the European ozone budget. J. Geophys. Res.-Atmos. 110https://doi.org/10.1029/2004jd005503. D11303.

Bell, M.L., Peng, R.D., Dominici, F., 2006. The exposure-response curve for ozone and risk of mortality and the adequacy of current ozone regulations. Environ. Health Perspect. 114, 532–536. https://doi.org/10.1289/ehp.8816.

Bell, M.L., Zanobetti, A., Dominici, F., 2014. Who is more affected by ozone pollution? A systematic review and meta-analysis. Am. J. Epidemiol. 180 (1), 15–28.

Brauer, M., Freedman, G., Frostad, J., van Donkelaar, A., Martin, R.V., Dentener, F., van Dingenen, R., Estep, K., Amini, H., Apte, J.S., Balakrishnan, K., Barregard, L., Broday, D., Feigin, V., Ghosh, S., Hopke, P.K., Knibbs, L.D., Kokubo, Y., Liu, Y., Ma, S.F., Morawska, L., Sangrador, J.L.T., Shaddick, G., Anderson, H.R., Vos, T., Forouzanfar, M.H., Burnett, R.T., Cohen, A., 2016. Ambient air pollution exposure estimation for the global burden of disease 2013. Environ. Sci. Technol. 50, 79–88. https://doi.org/10.1021/acs.est.5b03709.

Clifton, O.E., Fiore, A.M., Correa, G., Horowitz, L.W., Naik, V., 2014. Twenty-first century reversal of the surface ozone seasonal cycle over the northeastern United States. Geophys. Res. Lett. 41, 7343–7350. https://doi.org/10.1002/2014gl061378.

Colette, A., Granier, C., Hodnebrog, O., Jakobs, H., Maurizi, A., Nyiri, A., Bessagnet, B., D'Angiola, A., D'Isidoro, M., Gauss, M., Meleux, F., Memmesheimer, M., Mieville, A., Rouil, L., Russo, F., Solberg, S., Stordal, F., Tampieri, F., 2011. Air quality trends in Europe over the past decade: a first multi- model assessment. Atmos. Chem. Phys. 11, 11657–11678. https://doi.org/10.5194/acp-11-11657-2011.

Cooper, O.R., Gao, R.-S., Tarasick, D., Leblanc, T., Sweeney, C., 2012. Long-term ozone trends at rural ozone monitoring sites across the United States, 1990–2010. J. Geophys. Res. 117, D22307. https://doi.org/10.1029/2012JD018261.

Cooper, O.R., Parrish, D.D., Ziemke, J., Balashov, N.V., Cu- peiro, M., Galbally, I.E., Gilge,

S., Horowitz, L., Jensen, N.R., Lamarque, J.F., Naik, V., Oltmans, S.J., Schwab, J., Shindell, D.T., Thompson, A.M., Thouret, V., Wang, Y., Zbinden, R.M., 2014. Global distribution and trends of tropospheric ozone: an observation-based review. Elem. Sci. Anth. 2, 000029. https://doi.org/10.12952/journal.elementa.000029.

Derwent, R.G., Hjellbrekke, A.-G., 2013. In: Viana, M. (Ed.), Air Pollution by Ozone across Europe, Urban Air Quality in Europe. Springer.

Derwent, R.G., Witham, C.S., Utembe, S.R., Jenkin, M.E., Passant, N.R., 2010. Ozone in Central England: the impact of 20 years of precursor emission controls in Europe. Environ. Sci. Policy 13, 195–204. https://doi.org/10.1016/j.envsci.2010.02.001.

Derwent, R.G., Parrish, D.D., Galbally, I.E., Stevenson, D.S., Doherty, R.M., Young, P.J., Shallcross, D.E., 2016. Interhemispheric differences in seasonal cycles of tropospheric ozone in the marine boundary layer: observation-model comparisons. J. Geophys. Res.: Atmosphere 121, 11075–11085. https://doi.org/10.1002/2016JD024836.

EEA, 2009. Assessment of Ground-Level Ozone in EEA Member Countries, with a Focus on Long-Term Trends. vol. 56 European Environment Agency, Copenhagen.

EEA, 2017. Air Quality in Europe-2017 Report, EEA Report, No 13/2017, ISBN 978-92-9213-920-9. Publications Office of the European Union, Luxembourg, pp. 74. https://www.eea.europa.eu/publications/air-quality-in-europe-2017, Accessed date: 15 March 2018.

Escudero, M., Lozano, A., Hierro, J., del Valle, J., Mantilla, E., 2014. Urban influence on increasing ozone concentrations in a charac- teristic Mediterranean agglomeration. Atmos. Environ. 99, 322–332.

Fleming, Z.L., Doherty, R.M., von Schneidemesser, E., Malley, C.S., Cooper, O.R., Pinto, J.P., Colette, A., Xu, X.B., Simpson, D., Schultz, M.G., Lefohn, A.S., Hamad, S., Moolla, R., Solberg, S., Feng, Z.Z., 2018. Tropospheric Ozone Assessment Report: present-day ozone distribution and trends relevant to human health. Elem. Sci. Anth 6, 12. https://doi.org/10.1525/elementa.273.

Garcia Dos Santos, S., Benarroch Benarroch, R., Fernández Patier, R., Sintes Puertas, M.A., Cantón Gálvez, J.M., Alonso Herreros, J., Guevara Hernández, S., 2014. Atmospheric Pollution in North Africa. Facts and Lessons in the Spanish City of Ceuta, 9TH in-Ternational Conference on Air Quality Science and Application, 24–28 March 2014. Garmisch, Germany.

Guerreiro, C.B.B., Foltescu, V., de Leeuw, F., 2014. Air quality status and trends in Europe. Atmos. Environ. 98, 376–384. https://doi.org/10.1016/j.atmosenv.2014.09.017.

Hassler, B., McDonald, B.C., Frost, G.J., Borbon, A., Carslaw, D.C., Civerolo, K., Granier, C., Monks, P.S., Monks, S., Parrish, D.D., Pollack, I.B., Rosenlof, K.H., Ryerson, T.B., von Schneidemesser, E., Trainer, M., 2016. Analysis of long-term observations of NOx and CO in megacities and application to constraining emissions inventories. Geophys. Res. Lett. 43 (18), 9920–9930. https://doi.org/10.1002/2016GL069894.

Jenkin, M.E., 2008. Trends in ozone concentration distributions in the UK since 1990: local, regional and global influences. Atmos. Environ. 42, 5434–5445. https://doi.org/10.1016/j.atmosenv.2008.02.036.

Jöckel, P., Tost, H., Pozzer, A., Kunze, M., Kirner, O., Brenninkmeijer, C.A.M., Brinkop, S., Cai, D.S., Dyroff, C., Eckstein, J., Frank, F., Garny, H., Gottschaldt, K.-D., Graf, P., Grewe, V., Kerkweg, A., Kern, B., Matthes, S., Mertens, M., Meul, S., Neumaier, M., Nützel, M., Oberländer-Hayn, S., Ruhnke, R., Runde, T., Sander, R., Scharffe, D., Zahn, A., 2016. Earth System Chemistry integrated Modelling (ESCiMo) with the Modular Earth Submodel System (MESSy) version 2.51. Geosci. Model Dev. 9, 1153–1200. https://doi.org/10.5194/gmd-9-1153-2016.

Jonson, J.E., Simpson, D., Fagerli, H., Solberg, S., 2006. Can we explain the trends in European ozone levels? Atmos. Chem. Phys. 6, 51–66. https://doi.org/10.5194/acp-6-51-2006.

Kim, C.S., Alexis, N.E., Rappold, A.G., Kehrl, H., Hazucha, M.J., Lay, J.C., Schmitt, M.T., Case, M., Devlin, R.B., Peden, D.B., Diaz-Sanchez, D., 2011. Lung function and inflammatory responses in healthy young adults exposed to 0.06 ppm ozone for 6.6 hours. Am. J. Respir. Crit. Care Med. 183, 1215–1221. https://doi.org/10.1164/rccm.201011-1813OC.

Lamarque, J.-F., Bond, T.C., Eyring, V., Granier, C., Heil, A., Klimont, Z., Lee, D., Liousse, C., Mieville, A., Owen, B., Schultz, M.G., Shindell, D., Smith, S.J., Stehfest, E., Van Aar- denne, J., Cooper, O.R., Kainuma, M., Mahowald, N., Mc- Connell, J.R., Naik, V., Riahi, K., van Vuuren, D.P., 2010. Historical (1850–2000) gridded anthropogenic and biomass burning emissions of reactive gases and aerosols: methodology and ap- plication. Atmos. Chem. Phys. 10, 7017–7039. https://doi.org/10.5194/acp-10-7017-2010.

Lefohn, Allen S., Malley, Christopher S., Simon, Heather, Wells, Benjamin, Xu, Xiaobin, Zhang, Li, Wang, Tao, 2017. Responses of human health and vegetation exposure metrics to changes in ozone concentration distributions in the European Union, United States, and China. Atmos. Environ. 152, 123–145. https://doi.org/10.1016/j.atmosenv.2016.12.025.

Lelieveld, J., Dentener, F.J., 2000. What controls tropospheric ozone? J. Geophys. Res. 105, 3531–3551.

Lelieveld, J., Evans, J.S., Fnais, M., Giannadaki, D., Pozzer, A., 2015. The contribution of outdoor air pollution sources to premature mortality on a global scale. Nature 525, 367–371.

Lin, M., Fiore, A.M., Cooper, O.R., Horowitz, L.W., Langford, A.O., Levy II, H., Senff, C.J., 2012. Springtime high surface ozone events over the western United States: quantifying the role of stratospheric intrusions. J. Geophys. Res. 117, D00V22. https://doi.org/10.1029/2012JD018151.

Lin, M.Y., Horowitz, L.W., Cooper, O.R., Tarasick, D., Conley, S., Iraci, L.T., Johnson, B., Leblanc, T., Petropavlovskikh, I., Yates, E.L., 2015. Revisiting the evidence of increasing springtime ozone mixing ratios in the free troposphere over western North America. Geophys. Res. Lett. 42, 8719–8728. https://doi.org/10.1002/2015GL065311.

Lin, M.Y., Horowitz, L.W., Payton, R., Fiore, A.M., Tonnesen, G., 2017. US surface ozone trends and extremes from 1980 to 2014: quantifying the roles of rising Asian emissions, domestic controls, wildfires, and climate. Atmos. Chem. Phys. 17, 2943–2970. https://doi.org/10.5194/acp-17-2943-2017.

Eyring, V., Lamarque, J.-F., Hess, P., Arfeuille, F., Bowman, K., Chipperfield, M., Duncan, B., Fiore, A., Gettelman, A., Giorgetta, M., Granier, C., Hegglin, M., Kinnison, D., Kunze, M., Langematz, U., Luo, B., Martin, R., Matthes, K., Newman, P., Peter, T., Robock, A., Ryerson, A., Saiz-Lopez, A., Salawitch, R., Schultz, M., Shepherd, T., Shindell, D., Stähelin, J., Tegtmeier, S., Thomason, L., Tilmes, S., Vernier, J.-P., Waugh, D., Young, P., 2013. Overview of IGAC/SPARC Chemistry-Climate Model Initiative (CCMI) Community Simulations in Support of Upcoming Ozone and Climate Assessments. available at: http://www.sparc-climate.org/fileadmin/customer/6_Publications/Newsletter_PDF/40_SPARCnewsletter_Jan2013_web.pdf (last access: June 2017).

Monks, P.S., Archibald, A.T., Colette, A., Cooper, O., Coyle, M., Derwent, R., Fowler, D., Granier, C., Law, K.S., Mills, G.E., Stevenson, D.S., Tarasova, O., Thouret, V., von Schneidemesser, E., Sommariva, R., Wild, O., Williams, M.L., 2015. Tropospheric ozone and its precursors from the urban to the global scale from air quality to short-lived climate forcer. Atmos. Chem. Phys. 15, 8889–8973. https://doi.org/10.5194/acp-15-8889-2015.

Ordóñez, C., Elguindi, N., Stein, O., Huijnen, V., Flemming, J., Inness, A., Flentje, H., Katragkou, E., Moinat, P., Peuch, V.-H., Segers, A., Thouret, V., Athier, G., van Weele, M., Zerefos, C.S., Cammas, J.-P., Schultz, M.G., 2010. Global model simulations of air pollution during the 2003 European heat wave. Atmos. Chem. Phys. 10, 789–815. https://doi.org/10.5194/acp-10-789-2010.

Paoletti, E., De Marco, A., Beddows, D.C.S., Harrison, R.M., Manning, W.J., 2014. Ozone levels in European and USA cities are increasing more than at rural sites, while peak values are decreasing. Environ. Pollut. 192, 295e299.

Parrish, D.D., Law, K.S., Staehelin, J., Derwent, R., Cooper, O.R., Tanimoto, H., Volz-Thomas, A., Gilge, S., Scheel, H.E., Stein-bacher, M., Chan, E., 2013. Lower tropospheric ozone at northern midlatitudes: changing seasonal cycle. Geophys. Res. Lett. 40, 1631–1636. https://doi.org/10.1002/grl.50303.

Parrish, D.D., Lamarque, J.F., Naik, V., Horowitz, L., Shindell, D.T., Staehelin, J., Derwent, R., Cooper, O.R., Tanimoto, H., Volz-Thomas, A., Gilge, S., Scheel, H.E., Steinbacher, M., Frohlich, M., 2014. Long-term changes in lower tropospheric baseline ozone concentrations: comparing chemistry-climate models and observations at northern midlatitudes. J. Geophys. Res.: Atmosphere 119, 5719–5736. https://doi.org/10.1002/2013JD021435.

Parrish, D.D., Petropavlovskikh, I., Oltmans, S.J., 2017. Reversal of long- term trend in baseline ozone concentrations at the North American West Coast. Geophys. Res. Lett. 44, 10675–10681. https://doi.org/10.1002/2017GL074960.

Pawson, S., Steinbrecht, W., Charlton-Perez, A.J., Fujiwara, M., Karpechko, A.Y., Petropavlovskikh, I., Urban, J., Weber, M., 2014. Update on global ozone: past, present, and future. In: Scientific Assessment of Ozone Depletion: 2014, World Meteorological Organization, Global Ozone Research and Monitoring Project – Report No. 55, Chap. 2. World Meteorological Organization/UNEP.

Peng, R.D., Samoli, E., Pham, L., Dominici, F., Touloumi, G., Ramsay, T., Burnett, R.T., Krewski, D., Le Tertre, A., Cohen, A., Atkinson, R.W., Anderson, H.R., Katsouyanni, K., Samet, J.M., 2013. Acute effects of ambient ozone on mortality in Europe and North America: results from the APHENA study. Air Qual. Atmos. Health 6, 445–453. https://doi.org/10.1007/s11869-012-0180-9.

Pozzer, A., de Meij, A., Pringle, K.J., Tost, H., Doering, U.M., van Aardenne, J., Lelieveld, J., 2012. Distributions and regional budgets of aerosols and their precursors simulated with the EMAC chemistry-climate model. Atmos. Chem. Phys. 12, 961–987. https://doi.org/10.5194/acp-12-961-2012.

Querol, X., Alastuey, A., Pandolfi, M., Reche, C., Pérez, N., Min- guillón, M.C., Moreno, T., Viana, M., Escudero, M., Orio, A., Pallarés, M., Reina, F., 2014. 2001–2012 trends on air quality in Spain. Sci. Total Environ. 490, 957–969.

Querol, X., Alastuey, A., Orio, A., Pallares, M., Reina, F., Dieguez, J.J., Mantilla, E., Escudero, M., Alonso, L., Gangoiti, G., Millán, M., 2016. On the origin of the highest ozone episodes in Spain. Sci. Total Environ. 572, 379–389.

Sicard, P., De Marco, A., Troussier, F., Renou, C., Vas, N., Pao-letti, E., 2013. Decrease in surface ozone concentrations at Mediter- ranean remote sites and increase in the cities. Atmos. Environ. 79, 705–715.

Sicard, P., Serra, R., Rossello, P., 2016. Spatiotemporal trends in ground-level ozone concentrations and metrics in France over the time period 1999-2012. Environ. Res. 149, 122–144. https://doi.org/10.1016/j.envres.2016.05.014.

Simon, H., Reff, A., Wells, B., Xing, J., Frank, N., 2015. Ozone trends across the United States over a period of decreasing NOx and VOC emissions. Environ. Sci. Technol. 49, 186–195. https://doi.org/10.1021/es504514z.

Solberg, S., Hov, Ø., Søvde, A., Isaksen, I.S.A., Coddeville, P., De Backer, H., Forster, C., Orsolini, Y., Uhse, K., 2008. European surface ozone in the extreme summer 2003. J. Geophys. Res. 113, D07307. https://doi.org/10.1029/2007JD009098.

Staehelin, J., Tummon, F., Revell, L., Stenke, A., Peter, T., 2017. Tropospheric ozone at northern mid-latitudes: modeled and measured long- term changes. Atmosphere 8, 163. https://doi.org/10.3390/atmos8090163.

Tressol, M., Ordonez, C., Zbinden, R., Brioude, J., Thouret, V., Mari, C., Nedelec, P., Cammas, J.-P., Smit, H., Patz, H.-W., Volz-Thomas, A., 2008. Air pollution during the 2003 European heat wave as seen by MOZAIC airliners. Atmos. Chem. Phys. 8, 2133–2150. https://doi.org/10.5194/acp-8-2133-2008.

Vautard, R., Szopa, S., Beekmann, M., Menut, L., Hauglus- taine, D.A., Rouil, L., Roemer, M., 2006. Are decadal anthropogenic emission changes in Europe consistent with surface ozone observations? Geophys. Res. Lett. 33, L13810. https://doi.org/10.1029/2006GL026080.

Wang, T., Wei, X.L., Ding, A.J., Poon, C.N., Lam, K.S., Li, Y.S., Chan, L.Y., Anson, M., 2009. Increasing surface ozone concentrations in the background atmosphere of South- ern China, 1994–2007. Atmos. Chem. Phys. 9, 6217–6227. https://doi.org/10.5194/acp-9-6217-2009.

Weatherhead, E.C., Reinsel, G.C., Tiao, G.C., Meng, X.L., Choi, D.S., Cheang, W.K., Keller, T., DeLuisi, J., Wuebbles, D.J., Kerr, J.B., Miller, A.J., Oltmans, S.J., Frederick, J.E., 1998. Factors affecting the detection of trends: statistical considerations and applications to environmental data. J. Geophys. Res. Atmos. 103, 17149–17161. https://doi.org/10.1029/98jd00995.

Wilson, R.C., Fleming, Z.L., Monks, P.S., Clain, G., Henne, S., Konovalov, I.B., Szopa, S., Menut, L., 2012. Have primary emission reduction measures reduced ozone across Europe? An analysis of European rural background ozone trends 1996-2005. Atmos. Chem. Phys. 12, 437–454. https://doi.org/10.5194/acp-12-437-2012.

Xue, L.K., Wang, T., Gao, J., Ding, A.J., Zhou, X.H., Blake, D.R., Wang, X.F., Saunders, S.M., Fan, S.J., Zuo, H.C., Zhang, Q.Z., Wang, W.X., 2014. Ground-level ozone in four Chinese cities: precursors, regional transport and heterogeneous processes. Atmos. Chem. Phys. 14, 13175–13188. https://doi.org/10.5194/acp-14-13175-2014.

Yan, Y.-Y., Lin, J.-T., Chen, J., Hu, L., 2016. Improved simulation of tropospheric ozone by a global-multi-regional two-way coupling model system. Atmos. Chem. Phys. 16, 2381–2400. https://doi.org/10.5194/acp-16-2381-2016.

Yan, Y., Lin, J., He, C., 2018a. Ozone trends over the United States at different times of day. Atmos. Chem. Phys. 18, 1185–1202. https://doi.org/10.5194/acp-18-1185-2018.

Yan, Y.-Y., Pozzer, A., Ojha, N., Lin, J.-T., Lelieveld, J., 2018b. Analysis of European ozone trends in the period 1995–2014. Atmos. Chem. Phys. 18, 5589–5605. https://doi.org/10.5194/acp-18-5589-2018.

Yang, C.X., Yang, H.B., Guo, S., Wang, Z.S., Xu, X.H., Duan, X.L., Kan, H.D., 2012. Alternative ozone metrics and daily mortality in suzhou: the China air pollution and health effects study (CAPES). Sci. Total Environ. 426, 83–89. https://doi.org/10.1016/j.scitotenv.2012.03.036.

Yoon, J., Pozzer, A., 2014. Model-simulated trend of surface carbon monoxide for the 2001-2010 decade. Atmos. Chem. Phys. 14, 10465–10482. https://doi.org/10.5194/acp-14-10465-2014.

Young, P.J., Naik, V., Fiore, A.M., Gaudel, A., Guo, J., Lin, M.Y., Neu, J.L., Parrish, D.D., Rieder, H.E., Schnell, J.L., Tilmes, S., Wild, O., Zhang, L., Ziemke, J., Brandt, J., Delcloo, A., Doherty, R.M., Geels, C., Hegglin, M.I., Hu, L., Im, U., Kumar, R., Luhar, A., Murray, L., Plummer, D., Rodriguez, J., Saiz-Lopez, A., Schultz, M.G., Woodhouse, M.T., Zeng, G., 2018. Tropospheric Ozone Assessment Report: assessment of global-scale model performance for global and regional ozone distributions, variability, and trends. Elem. Sci. Anth 6, 10. https://doi.org/10.1525/elementa.265.

Zervas, E., 2006a. CO2 benefit from the increasing percentage of diesel passenger cars. Case of Ireland. Energy Policy 34 (17), 2848–2857. https://doi.org/10.1016/j.enpol.2005.05.010.

Zervas, E., Poulopoulos, S., Philippopoulos, C., 2006b. CO2 emissions change from the introduction of diesel passenger cars: case of Greece. Energy 31 (14), 2915–2925. https://doi.org/10.1016/j.energy.2005.11.005.

Ziemke, J.R., Oman, L.D., Strode, S.A., Douglass, A.R., Olsen, M.A., McPeters, R.D., Bhartia, P.K., Froidevaux, L., Labow, G.J., Witte, J.C., Thompson, A.M., Haffner, D.P., Kramarova, N.A., Frith, S.M., Huang, L.-K., Jaross, G.R., Seftor, C.J., Deland, M.T., Taylor, S.L., 2018. Trends in global tropospheric ozone inferred from a composite record of TOMS/OMI/MLS/OMPS satellite measurements and the MERRA-2 GMI simulation. Atmos. Chem. Phys. Discuss submitted for publication. https://doi.org/10.5194/acp-2018-716.